Carbon – Science and Technology

ISSN 0974 – 0546

http://www.applied-science-innovations.com

RESEARCH ARTICLE Received: 27/04/2017, Accepted: 04/06/2017

Sonochemical synthesis & characterization of Dy^{3+} capped $MgSiO_3$ nanostructures and their photoluminescence studies for display device application

G. R. Revannasiddappa[1,2,*], M. S. Rudresha[2], H. Nagabhushana[3], R. B. Basavaraj[3], and B. Daruka prasad[4]

1) Sree Siddaganga College of Arts, Science & Commerce for Women, Tumkur-572102, India.
2) Sri Siddhartha Academy of Higher Education, Agalakote, Tumkur-572105, India.
3) Prof. C.N.R. Rao Centre for Advanced Materials, Tumkur University, Tumkur- 572103, India.
4) Department of Physics, B.M.S Institute of Technology and Management, Yelahanka, Bangalore-560064, India.

*Corresponding author: grrevannasiddappa@gmail.com (G.R. Revannasiddappa).

Abstract: A simple bio-template assisted ultrasound synthesis method is followed for the preparation of pure and Dy^{3+} (1-11 mol %) doped $MgSiO_3$ nanophosphors. Various experimental parameters influences in controlling the shape, size and morphology of the obtained products. The final product is well characterized by powder X-ray diffraction (PXRD), scanning electron microscopy (SEM), transmission electron microscopy (TEM) and photoluminescence (PL). It is noticed that the morphology of the product was highly dependent on the surfactant (*mimosa pudica*) concentration, sonication time, pH and sonication power. The formation mechanism for various micro/nano superstructures is proposed. The characteristic photoluminescence peaks are observed at 484, 574 and 666 nm due to the electronic transitions $^4F_{9/2} \rightarrow {}^6H_j$ (j=15/2, 13/2, 11/2) of Dy^{3+} ions upon excited at wavelength of 350 nm [$^6H15/2 \rightarrow {}^6P_{7/2}$ ($^4M_{15/2}$)]. The photometric studies indicate that the obtained phosphors may be promising compounds in white light emitting diodes (wLED's). The present synthesis route is rapid, environmentally benign, cost effective and useful for industrial applications such as solid state lighting and display devices.

Keywords: Sonochemical synthesis; Nanophosphor; Photoluminescence; bio-surfactant.

1 Introduction: White light-emitting diodes (WLEDs) have emerged as the next generation of illumination technology. LEDs were considered to be the light source that will replace the conventional incandescent and fluorescence lamps, due to high luminous efficiency, long life time, energy saving, harmlessness, easy fabrication, high stability and environmental safety [1]. Rare earth ions activated phosphors have attracted much attention of many scientists due to their unique electronic, optical and chemical properties resulted from the 4f shell of the ion; and the progress in the development of the phosphors is directly related to the understanding of the physical processes of energy absorption and relaxation [2–4]. Therefore, the f–f transitions of the trivalent lanthanide ions in crystalline hosts is receiving more attention as optical materials emitting in the visible and near-IR regions [5, 6]. Among rare earth ions, Dy^{3+} is one of the most investigated ions, and it has been studied extensively because it provides two typical emission bands in blue (480 nm) and yellow (570 nm) regions, which are necessary for full color displays [7–9]. In addition, the emission probability of electric dipole transition is greatly

affected by the crystal field and radial integral of 4f and 5d electrons. Therefore, it is interesting to study the luminescence properties of Dy^{3+} in different host lattices. Due to its excellent chemical and thermal stability, long persistence time, better formability, multicolor phosphorescence, easy preparation, resistance for alkali and oxygen, silicate is considered to be one of the best host materials for luminescence centers **[10, 11]**. When doped with rare-earth ions or transition metal ions, silicate becomes phosphor material, which produces intense luminescence in the blue, green and red emission peak **[12, 13]**. However, the shape and size of nanoparticles depend on their synthesis method. For the preparation of nano materials, a variety of methods were designed, including templating method **[14]**, sol–gel reaction **[15]**, hydrothermal technology **[16]**, solution combustion route **[17]**, etc. Among the reported synthesis techniques, the solution combustion route was a low-cost, time saving and high-yield approach.

Recently, rare earth metal ion doped oxide hosts find large number of applications including luminescent materials, catalysts, photonic applications, displays, thermo luminescence dosimetry, etc. **[18, 19]**. Rare earth dysprosium ions attracted considerable attention because of their white light emission. It was well-known that a Dy^{3+} ion with a $^4f_9$ electron configuration generally shows two dominant emission color bands of the luminescence which was close to white light because of its visible emission bands including a blue emission of ~480nm and a yellow emission of ~574 nm **[20, 21]**. Therefore, it was possible to obtain white light from Dy^{3+} ion activated luminescent materials by adjusting the intensity ratio of yellow to blue emissions by choosing different hosts.

In this paper we report a facile ultrasound assisted sonochemical route for the synthesis of pure and Dy^{3+} doped $MgSiO_3$ nanophosphors using bio-surfactant (*mimosa pudica*). Effect of various reaction conditions, structural, morphological and optical studies were carried out in detail.

2. Experimental

2.1. Materials and methods: Pure and Dy^{3+} (1 - 11 mol %) doped $MgSiO_3$ nano/micro structures were synthesized by using *mimosa pudica* as a bio-template surfactant via ultrasound method. The precursor solutions of Magnesium nitrate [$Mg(NO_3)_2$], Dysprosium nitrate [$Dy(NO_3)_2$] were prepared by dissolving stoichiometric quantities of both the nitrates separately in 50 ml of double distilled water and then mixed the solutions after obtaining the clear solution. 5 ml of *mimosa pudica* leaves extract was mixed in 100 ml double distilled water and added to the resultant mixture slowly. Then, the solution products was stirred ultrasonically (ultrasonic frequency ~ 20 kHz, power ~ 300 W) at fixed temperature of 333 K and by varying the sonication time (1 - 6 h). Once the white precipitate was formed, the precipitate was filtered and washed by using distilled water and ethanol to remove any unwanted content in the mixture. The final precipitated powder was dried at 333 K for 3 h in a vacuum oven and used for further studies.

2.2. Characterization: The powder X-ray diffraction (PXRD) measurements were made using Shimadzu made model-7000, having a high precision vertical θ–θ goniometer and Cu-K_α radiation with a wavelength of 1.54 Å. Morphology of the NPs and size of the particles were examined by scanning electron microscope (SEM, Hitachi-3000) and transmission electron microscope (TEM, TECNAI F-30) respectively. Photoluminescence (PL) measurements were carried out using Horiba Fluorolog-3, modular Spectroflourimeter.

3. Results and discussion

3.1 PXRD analysis: Debye – Scherrer's equation and Williamson and Hall method were employed to determine the average crystallite sizes of pure and Dy^{3+} doped $MgSiO_3$ nanophosphor from the XRD pattern shown in Figure (1) **[22]**.

$$D = \frac{0.9\,\lambda}{\beta \cos\theta} \qquad \text{----- (1)}$$

where 'β'; the diffracted full width at half maximum (FWHM in radian) caused by the crystallites, 'λ'; the wavelength of X-ray (1.542 Å), 'θ'; the Bragg angle and k; is the constant depends on the grain shape (0.90).

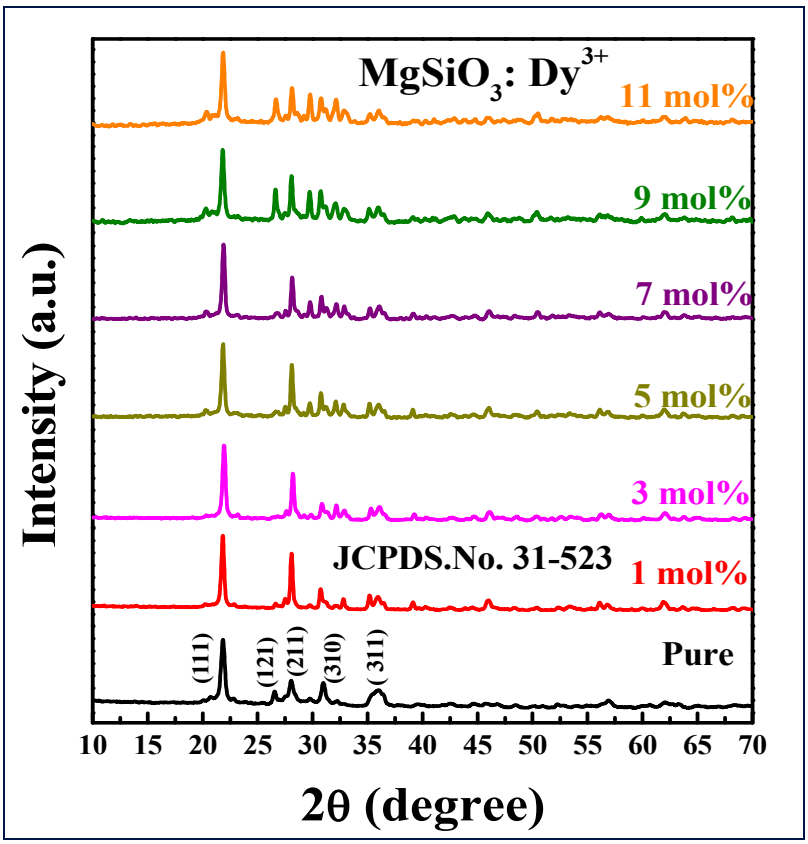

Figure (1): PXRD patterns of pure & Dy^{3+} (1-11 mol %) doped $MgSiO_3$ nanophosphors.

The W – H approach considers the case when the domain effect and lattice deformation were both simultaneously operative and their combined effects give the final line broadening FWHM (β), which is the sum of grain size and lattice distortion. This relation assumes a negligibly small instrumental contribution compared with the sample – dependent broadening. W – H equation may be expressed in the form:

$$\beta \cos\theta = \varepsilon\left(4 \sin\theta\right) + \frac{\lambda}{D} \qquad \text{--------- (2)}$$

Where 'β' (FWHM in radians) is measured for different XRD lines corresponding to different planes ε; the strain developed and D; the grain size. The equation represents a straight line between 4 sinθ (X – axis) and β cosθ (Y – axis) for host and $MgSiO_3$: Dy^{3+} (1-11 mol %) nanomaterials (Figure 2). The slope of the line gives the strain (ε) and intercept (λ / D) of this line on the Y – axis gives grain size (D). The crystallite size estimated from W- H plots is slightly higher than those calculated using Scherrer's relation. The small variation in the values were due to the fact that in Scherrer's formula strain component is assumed to be zero and observed broadening of diffraction peak is considered as a result of reducing grain size only.

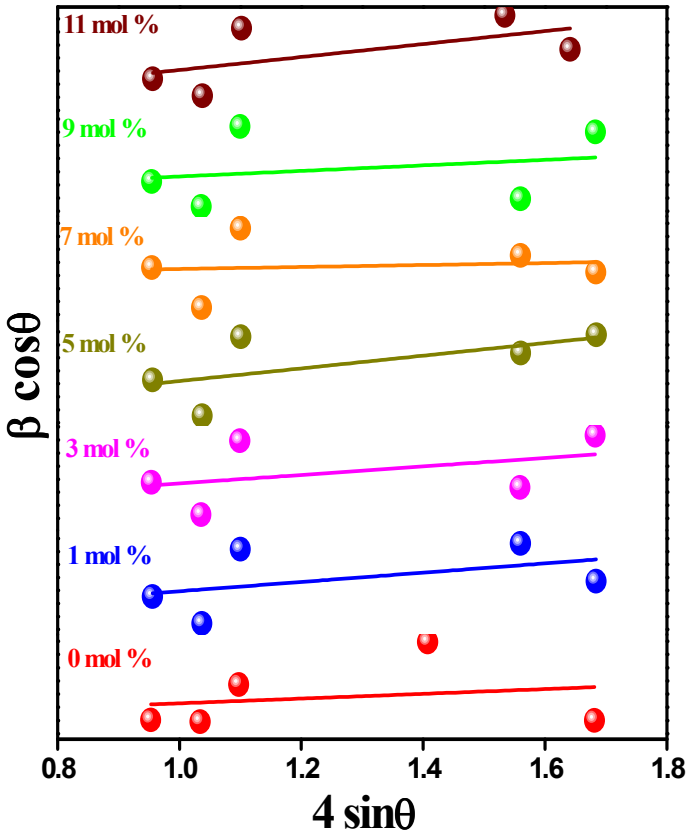

Figure (2): W-H plots of pure & Dy^{3+} (1-11 mol %) doped $MgSiO_3$ nanophosphors.

The other structural parameters; dislocation density (δ) and stacking fault (SF) is determined using the following relation:

$$\delta = \frac{1}{D^2} \qquad \text{……..(3)}$$

$$SF = \left[\frac{2\pi^2}{45\,(3\tan\theta)^{1/2}} \right] \qquad \text{------- (4)}$$

The estimated average crystallite size, strain, dislocation density and stacking fault for host and $MgSiO_3$: Dy^{3+}nanophosphor were tabulated in Table (1).

Table (1): Estimated crystallite size, strain, dislocation density and stacking fault values of un-doped and Dy^{3+} doped $MgSiO_3$ nanophosphor.

$MgSiO_3$: Dy^{3+} (mol %)	Average crystallite size d (nm)		Micro-strain ε (x 10^{-3})	Lattice strain ϵ (10^{-3})	Dislocation density δ (10^{14} lin m^{-2})	Stacking fault
	Scherrer's method	W-H Plots				
0	40	40	1.01	3.39	6.21	0.48
1	31	43	1.11	3.19	9.88	0.45
3	31	39	1.09	3.47	9.79	0.47
5	31	42	1.12	3.29	10.17	0.43
7	30	31	1.15	4.39	10.74	0.42
9	33	35	1.11	3.89	8.96	0.43
11	30	41	1.02	2.24	10.48	0.41

3.2 Morphological analysis: Figure (3) shows the SEM micrographs of $MgSiO_3$:Dy^{3+} (5 mol %) nanophosphors with 30 ml of *mimosa pudica* surfactant concentration at different ultrasonic irradiation time (1-4 h). When the ultrasonic irradiation time is 1 h, clusters with uneven shaped microstructures were obtained. As the sonication time is increased to 2 h these clusters diffuse with each other and form a network of fibers in all the directions. When the sonication time was increased to 3 & 4 h there will be formation of sharp needle like structures directed outwards were observed. These sharp needles were clearly observed directed outwards from the nanocluster mesh at higher sonication time. From these different type of morphology we can predict that the reaction parameter like sonication time and surfactant concentration play a key role in controlling the morphology of the product.

Figure (4) shows the TEM and HRTEM images of $MgSiO_3$:Dy^{3+} (5 mol %) nanophosphors. From the images it is found that the d spacing value is 0.29 nm. These results were in good agreement with the crystallite size calculated from the W-H plots.

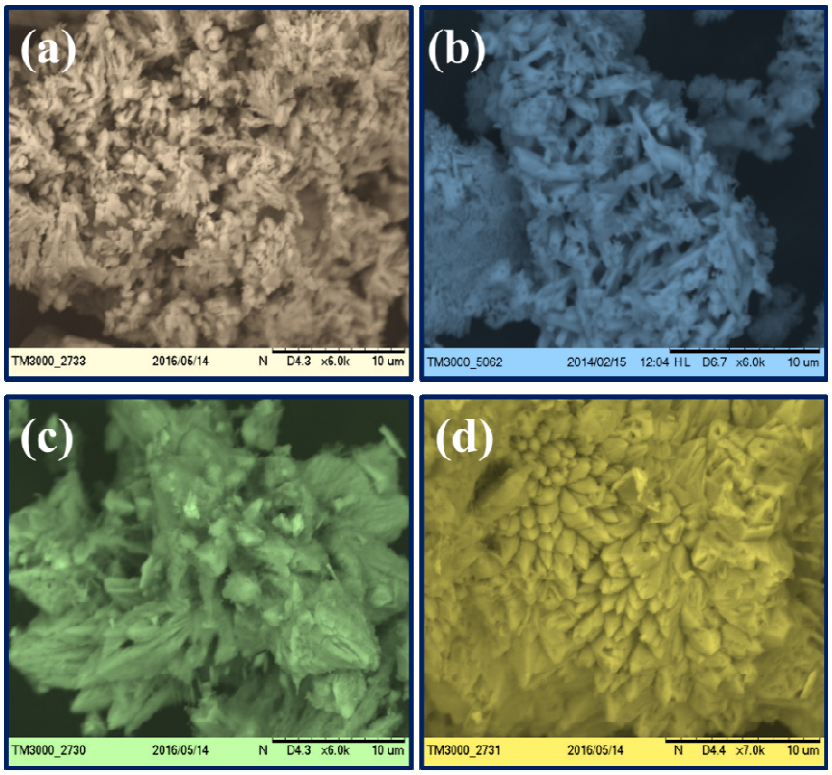

Figure (3): SEM micrographs of $MgSiO_3:Dy^{3+}$ nanophosphors with different sonication time with 30 ml of *mimosa pudica*. (a) 1hr, (b) 2hr, (c) 3hr, (d) 4hr.

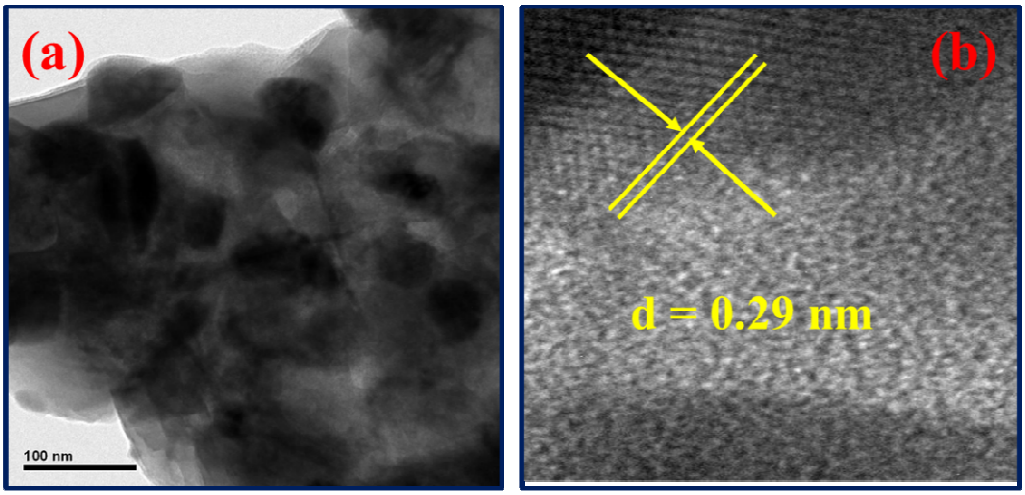

Figure (4): TEM & HRTEM images of $MgSiO_3:Dy^{3+}$ (5 mol %) nanophosphors.

3.3 Photoluminescence studies: Figure (5) shows excitation spectrum of $MgSiO_3$: Dy^{3+} (3 mol %) nanophosphor obtained by monitoring the emission of the $^4F_{9/2} \rightarrow {}^6H_{13/2}$ transition of Dy^{3+} ion. The excitation spectrum consist a sharp intense band at 350 nm corresponding to $^6H_{15/2} \rightarrow {}^6P_{7/2} + {}^4M_{17/2}$ transition attributed to the direct excitation of Dy^{3+} ion.

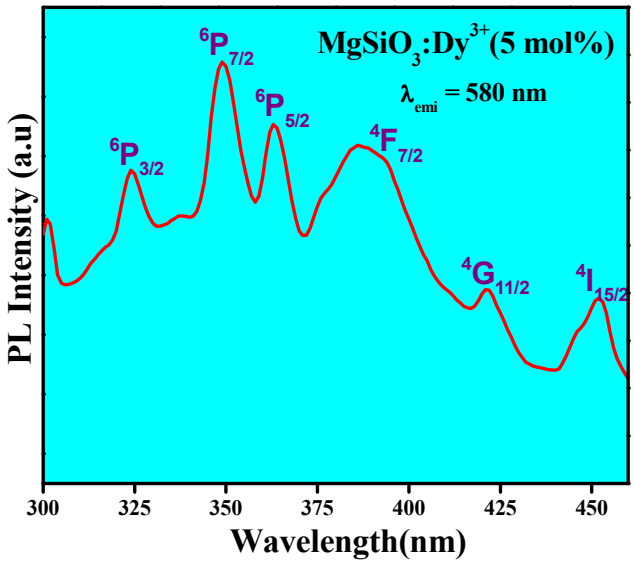

Figure (5): Excitation spectrum of $MgSiO_3$: Dy^{3+} (5 mol %) nanophosphors.

Under 350 nm excitation, namely exciting the Dy^{3+} ions to the $^6P_{5/2}$ multiplet, emission spectra in the range 400 - 700 nm were recorded as shown in Figure (6). According to energy level positions of Dy^{3+} ions the emission bands observed around 480, 574, and 666 nm were attributed to the $^5F_{9/2} \rightarrow {}^6H_J$ (J = 15/2, 13/2 and 11/2) transitions respectively. Among these, transitions, $^4F_{9/2} \rightarrow {}^6H_{13/2}$ are purely electric dipole (ED) transitions but the $^4F_{9/2} \rightarrow {}^6H_{15/2}$ obey magnetic dipole (MD) transitions A MD transition does not change with the host environment significantly but the ED transition is sensitive to the crystal field [23].

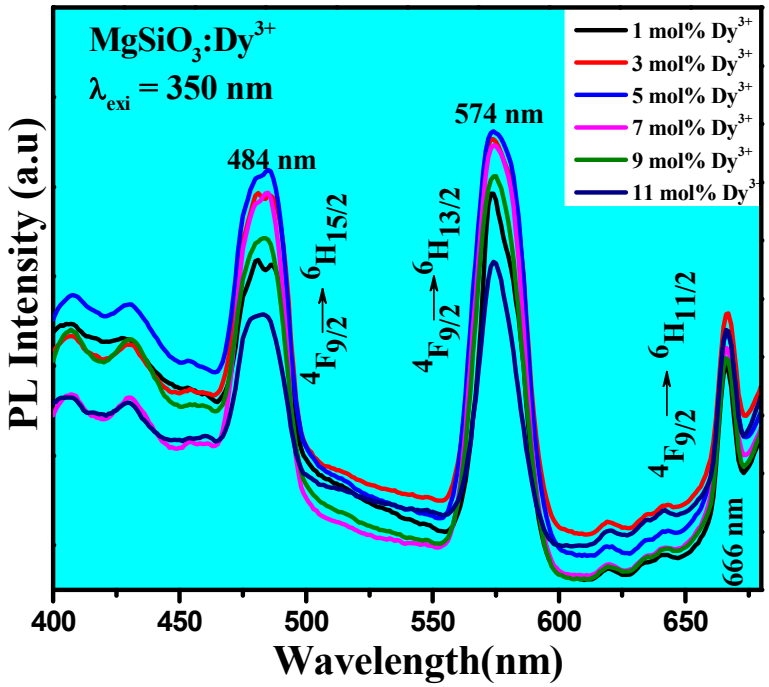

Figure (6): Emission spectra of $MgSiO_3$: Dy^{3+} (1-11 mol %) nanophosphors.

It was observed that maximum emission intensity of $MgSiO_3$: Dy^{3+} phosphor appear at 5 mol %. At higher concentration (> 5 mol %), the luminescence intensity reduces contrarily owing to concentration quenching effect. The concentration quenching occurs due to the energy transfer from one activator to

the neighboring ion. The critical distance for energy transfer (Rc) in $MgSiO_3$: Dy^{3+} NPs was estimated from the structural parameters namely unit cell volume (V), total Dy^{3+} sites per unit cell (N) and critical concentration (Xc) [24].

$$R_c \approx 2\left[\frac{3V}{4X_c \pi N}\right]^{1/3} \quad \text{----- (5)}$$

For the $MgSiO_3$: Dy^{3+}system, $N = 4$, $V = 786$ (Å) ^{3} and $X_c = 0.03$. The R_c of Dy^{3+} ions in $MgSiO_3$ were found to be ~ 10.245Å. When critical energy distance between Dy^{3+} ion in $MgSiO_3$ is greater than 5 Å, the overlapping between excitation and emission spectra decreases. The energy transfer between Dy^{3+}ion take places due to electric multipolar interaction which can be determined by the equation:

$$\frac{I}{X} = k\left[1+\beta (X)^{Q/3}\right]^{-1} \quad \text{------- (6)}$$

where X; Dy^{3+} ion concentration, k and β; constants, Q = 6, 8 and 10 for dipole – dipole, dipole – quadruple and quadruple – quadruple interactions. The value of Q is determined by plotting log (X) *Vs* log (I/X) (Figure 7) which gives a linear graph having a slope = - 1.5892 and intercept = 8.0129 The Q value is close to 6 indicates that the concentration quenching in $MgSiO_3$ is due to dipole- dipole interaction [25].

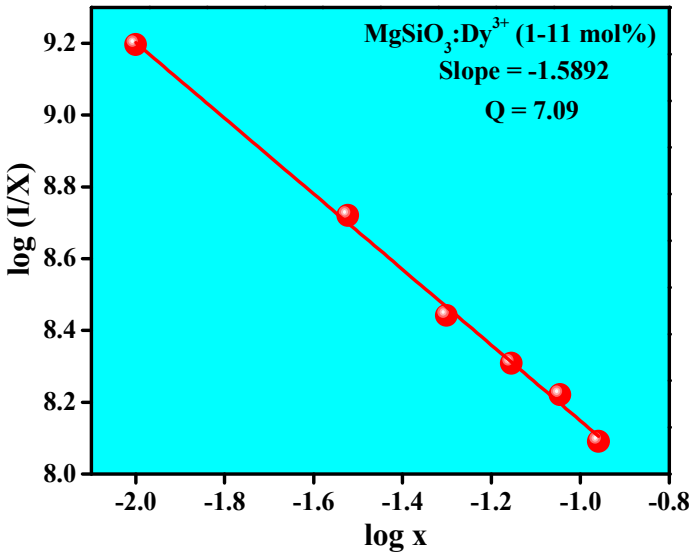

Figure (7): Log x vs log I/X for 574 nm peak.

Commission International de I'Eclairage (CIE) 1931 x-y chromaticity diagram of $MgSiO_3$: Dy^{3+} (1-11 mol %) nanophosphors were presented in Figure (8) excited under 350 nm. As shown in the inset of Figure (8), the CIE chromaticity coordinates were located in the white region. To identify technical applicability of this white emission, Correlated color temperature (CCT) is determined from CIE coordinates. Figure (9) shows the CCT diagram of $MgSiO_3$: Dy^{3+} (1-11 mol %) nanophosphors excited under 350 nm. The CCT is a specification of the color appearance of the light emitted by a light source, relating its color to the color of light from a reference source when heated to particular temperature. However, lamps with a CCT rating below 3200 K are usually considered as "warm" light sources, while those with a CCT above 4000 K are usually considered as "cool" in appearance. In the present study, the CCT of $MgSiO_3$: Dy^{3+}nanophosphorwas found to be 6272 K which is within the range of vertical daylight. Thus it can be useful for artificial production of illumination devices [26].

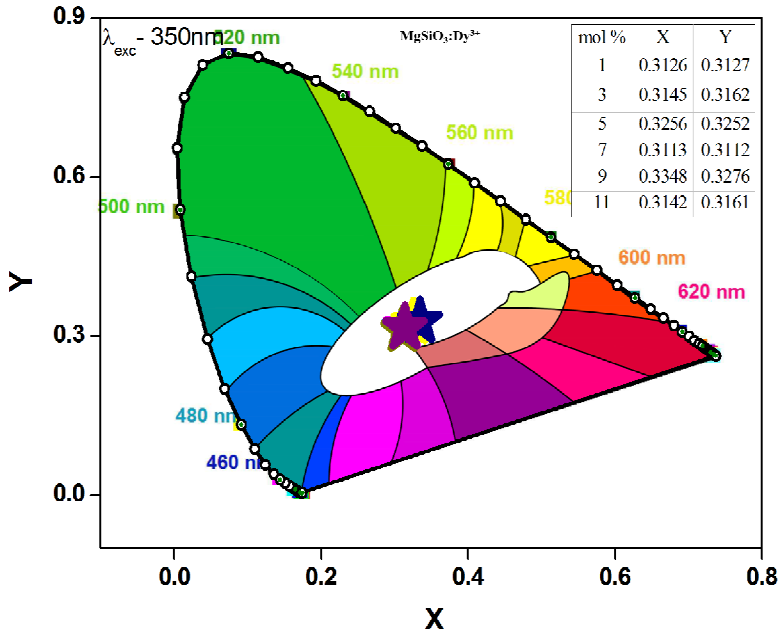

Figure (8): CIE chromaticity diagram of (1–11 mol %) Dy^{3+} doped $MgSiO_3$ nanophosphor.(Inset: Values of X & Y used for CIE studies).

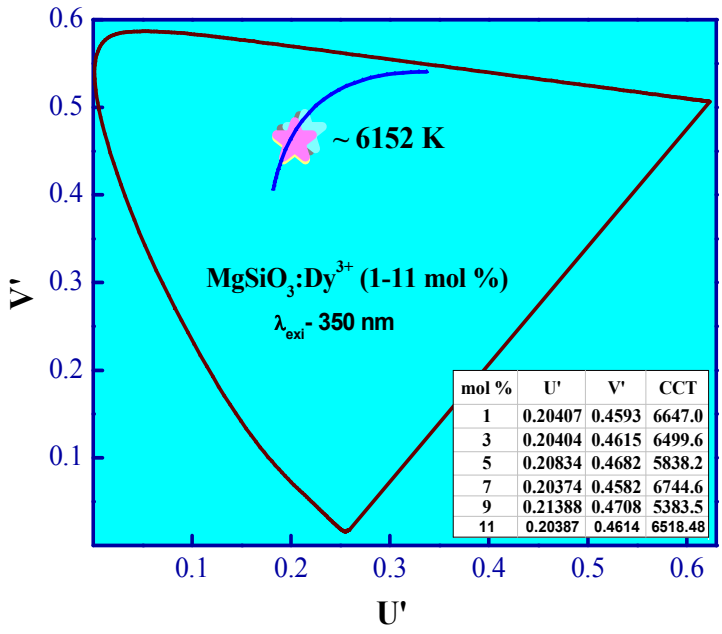

Figure (9): Correlated color temperature (CCT) diagram of (1–11 mol %) Dy^{3+} doped $MgSiO_3$ nanophosphor. (Inset: U□ ,V□ values for calculating CCT values).

4 Conclusions: For the first time, pure and Dy^{3+} (1-11 mol %) $MgSiO_3$ nanostructures were prepared successfully by ultrasound assisted sonochemical route using bio-template *mimosa pudica* as surfactant. The method followed has several benefits such as low cost, energy efficiency, high production volume and above all, easy method of preparation. From PXRD studies a single monoclinic phase was achieved. The crystallite size was estimated were in the range 30 – 40 nm respectively. From SEM studies, the

particles appear to be non-uniform and agglomerates composed of circular with several micrometers in size. PL spectra consist of three main groups of peaks in 450–500 nm (blue), 550–600 nm (yellow) and 666 nm (red) respectively. These peaks were assigned to transition of $^5F_{9/2} \rightarrow {}^6H_J$ (J = 15/2, 13/2 and 11/2). The chromaticity co-ordinates of all the prepared phosphors were located in white light. Therefore, Dy^{3+} activated $MgSiO_3$ was a promising single phased phosphor for WLED's.

Acknowledgement: The author G.R. Revannasiddappa thanks to UGC (Project No. 1513-MRP/14-15/KATU008/UGC-SWRO) University Grant Commission, Bangalore for the sanction of this Project.

References

[1] Shaodong Su, Wei Liu, Ruijing Duan, Lixin Cao, Ge Su, Chenggong Zhao, J. Alloys Compd. 575 (2013) 309–313.
[2] C. F. Wu, W. P. Qin, G. S. Qin, D. Zhao, J. S. Zhang, S. H. Huang, S. Z. Lv, H. Q. Liu, H. Y. Lin, Appl. Phys. Lett. 82 (2003) 520–522.
[3] J. Dexpert Ghys, R. Mauricot, M. D. Faucher, J. Lumin. 69 (1996) 203-215.
[4] B. Bihari, H. Eilers, B. M. Tissue, J. Lumin. 75 (1997) 1–10.
[5] B. Li, Z. N. Gu, J. H. Lin, M. C. Su, Chem. J. Chin. Univ. 22 (2001) 1-5.
[6] Z. H. Jia, H. Li, Z. R. Ye, Chem. J. Chin. Univ. 23 (2002) 352–353.
[7] J. Y. Kuang, Y. L. Liu, Chem. Lett. 34 (4) (2005) 598–599.
[8] Y. L. Liu, B. F. Lei, C. S. Shi, Chem. Mater. 17 (8) (2005) 2108–2113.
[9] B. Liu, L. J. Kong, C. S. Shi, J. Lumin. 121 (2007) 122–123.
[10] L. Jiang, C. K. Chang, D. L. Mao, C. L. Feng, Opt. Mater. 27 (2004) 51–55.
[11] Y. Liu, C. N. Xu, H. Matsui, T. Imamura, T. Watanabe, J. Lumin. 87–89 (2000)1297–1299.
[12] N. V. Kuleshov, V. P. Mikhailov, V. G. Scherbitsky, B. I. Minkov, T. J. Glynn, R. Sherlock, Opt. Mater. 4 (1995) 507–513.
[13] X. P. Fan, M. Q. Wang, Y. Yu, Q. Z. Wu, J. Phys. Chem. Solids 57 (9) (1996)1259–1262.
[14] J. G. Yu, W. Liu, H. G. Yu, Cryst. Growth Des. 8 (3) (2008) 930–934.
[15] W. S. Yang, Z. G. Teng, Y. D. Han, J. Li, F. Yan, Mater. 127 (1–2) (2010) 67–72.
[16] Qian Zhang, Wei Li, Shouxin Liu, Powder Technol. 212 (2011) 145–150.
[17] P. B. Devaraja, D. N. Avadhani, S. C. Prashantha, H. Nagabhushana, S. C. Sharma, B. M. Nagabhushana, H. P. Nagaswarupa, Spectrochim. Acta A Mol. Biomol. Spectrosc.118 (2014) 847–851.
[18] J. Li, G. Lu, B. Xie, Y. Wang, Y. Guo, Y. Guo, J. Rare Earths 30 (2012) 1096–1101.
[19] B. M. E. Russbueldt, W. F. Hoelderich, J. Catal. 271 (2010) 290–304.
[20] Feng Gu, Chunzhong Li, Hongming Cao, Wei Shao, Yanjie Hu, Jitao Chen, Aiping Chen, J. Alloys Compd. 453 (2008) 361–365.
[21] S. C. Prashantha, B. N. Lakshminarasappa, Fouran Singh, Curr. Appl. Phys.11 (2011) 1274–1277.
[22] S. C. Prashantha, B. N. Lakshminarasappa, Fouran Singh, J. Lumin.132 (2012) 3093–3097.
[23] R. B. Basavaraj H. Nagabhushana B. Daruka Prasad, S. C. Sharma S. C. Prashantha B. M. Nagabhushana, Optik. 126 (2015) 1745-1756.
[24] Y. S. Vidya, K. Gurushantha, H. Nagabhushana, S. C. Sharma, K. S. Anantharaju, C. Shivakumara, D. Suresh, H. P. Nagaswarupa, S. C. Prashantha, M. R. Anilkumar, J. Alloys. Compd. 622 (2015) 86-96.
[25] B. S. Ravikumar, H. Nagabhushana, S. C. Sharma, Y. S. Vidya, K. S. Anantharaju, Spectrochemica Acta A, 136 (2015) 1027-1037.
[26] S. D. Meetei, S. D. Singh, J. Alloys Compd. 587 (2014) 143-147.

*****